Journal of the Serbian Chemical Society

JSCS-info@shd.org.rs • www.shd.org.rs/JSCS

J. Serb. Chem. Soc. 80 (2) 197–207 (2015)
JSCS–4710

UDC 546.73–72+544.654.2:621.397.3+
621385.833:537.621
Original scientific paper

Correlation between morphology and magnetic properties of electrochemically produced cobalt powder particles

VESNA M. MAKSIMOVIĆ[1]*, NEBOJŠA D. NIKOLIĆ[2#], VLADAN B. KUSIGERSKI[1] and JOVAN L. BLANUŠA[1]

[1]*Institute of Nuclear Sciences, "Vinča", University of Belgrade, P. O. Box 522, 11001 Belgrade, Serbia and* [2]*ICTM – Institute of Electrochemistry, University of Belgrade, Njegoševa 12, P. O. Box 473, 11001 Belgrade, Serbia*

(Received 20 August, revised 8 October 2014, accepted 24 October 2014)

Abstract: Cobalt 3D powder particles were successfully prepared by galvanostatic electrodeposition. The electrodeposited cobalt powders were characterized by X-ray diffraction (XRD) analysis, scanning electron microscopy (SEM), energy dispersive spectroscopy (EDS) and SQUID magnetometry. It was shown that the morphology, structure and magnetic properties of cobalt particles were closely associated and could be easily controlled by adjusting the electrodeposition process parameters. The morphology of cobalt powder particles was strongly affected by the hydrogen evolution reaction as a parallel reaction to cobalt electrodeposition. Depending on the applied current density, two types of powder particles were formed: dendrites at lower and spongy-like particles at higher current densities. Morphologies and structures of powder particles were correlated with their magnetic properties, and compared with those of the bulk cobalt. In comparison with the properties of bulk cobalt, the obtained 3D structures exhibited a decreased saturation magnetization (M_S), but an enhanced coercivity (H_C), which was explained by their peculiar morphology.

Keywords: electrodeposition; cobalt; powder; scanning electron microscope; X-ray diffraction analysis; magnetic properties.

INTRODUCTION

Due to its specific physical properties, ferromagnetic cobalt has received attention in both basic scientific research and technological applications, such as, for example, in high-density information storage, magnetic sensors, *etc*.[1] The fact that the crystal structure and magnetic properties of cobalt are considerably susceptible to particle size and morphology led to development of numerous syn-

* Corresponding author. E-mail: vesnam@vinca.rs
# Serbian Chemical Society member.
doi: 10.2298/JSC200814104M

thetic methods aimed at obtaining specific particle sizes/shapes. These methods included thermal decomposition of cobalt carbonyl and organometallic precursors, template-mediated synthesis, solvothermal and electrodeposition methods. Various morphological forms, such as wires, rods, disk, ring and tree-like cobalt, were successfully synthesized by some of these methods.[2–7]

The crystal structure of cobalt in its bulk form comprises two allotropes, *i.e.*, hexagonal close packed (hcp) and face centred cubic (fcc). The transition from the hcp to the fcc phase can be temperature induced so that the hcp structure is stable at room temperature, while the fcc phase becomes stable at temperatures above approximately 450 °C.[8] It was shown that with reduction in the grain size, the fcc-phase becomes the more stable phase at ambient conditions,[9] although the hcp structure can also be stabilized for nano-sized cobalt under special synthesis conditions.[10,11] In addition, in the nanometre size range, a new metastable phase can also appear, called ε-Co, with properties between the hcp and fcc phases.[12]

From the viewpoint of magnetism, bulk cobalt is a well known ferromagnetic material with the high Curie temperature close to $T_C \approx 1390$ °C.[13] However, hcp-Co is magnetically much harder than fcc-Co, meaning that the coercivity field H_C^{hcp} can be up to an order of magnitude higher than H_C^{fcc}, while the saturation magnetization values M_S of both phases are virtually the same.[13] In practice, the majority of bulk cobalt samples consist of mixed hexagonal and cubic phases[14] so that typical H_C values amount few tens of Oe* while typical M_S values are around 168 emu g^{-1}.

Electrodeposition is very valuable method to obtain a metal in the desired form suitable for applications in the above-mentioned technologies. Morphology, as the most important property of electrodeposited metal, mainly depends on the electrodeposition conditions, such as regime of electrolysis, composition of the solution, type of working electrode and temperature, and the nature of the metal.[15,16] Cobalt belongs to the group of inert metals, together with Fe, Ni, Mn, Cr and Pt.[17] The characteristics of these metals are high melting points, low exchange current densities and low overpotentials for hydrogen discharge. Due to these characteristics, electrodeposition of cobalt occurs together with the hydrogen evolution reaction, enabling the formation of cobalt in powder form over a wide range of potentials and current densities.

For this reason, in the present study, this method was used to produce cobalt 3D powder particles of different surface morphology. The powder particles obtained in the galvanostatic regime of electrolysis were analyzed with respect to their morphology, structure and magnetic properties.

* 1 Oe$\times 10^3/4\pi$ = 1 A/m; 1 emu/g = 1 A m^2/kg

EXPERIMENTAL

Cobalt powders were electrodeposited from the electrolyte containing 0.10 M $CoSO_4$ + + 0.70 M NH_4OH + 1.0 M $(NH_4)_2SO_4$ at a current density of 500 mA cm^{-2} and a current density which corresponded to the limiting diffusion current density of 770 mA cm^{-2}. All chemical reagents in this work were of analytical grade purity. Electrolytes were made from chemicals and pure water (EASY pure UV, 18.3 MΩ, Barnstead). The working electrode was glassy carbon, while the counter electrode was pure platinum.

Cobalt powder samples were electrodeposited at the room temperature in a cylindrical glass cell with a cone-shaped bottom in order to collect the powder particles. The total volume of the cell was 1 dm^3. During the deposition process, the powder was not removed from the electrode surface, but was left to self-detach. After deposition, the powders were washed with EASY pure UV water and ethanol, and left to dry in the air at room temperature.

The morphology of the electrodeposited powders was examined using scanning electron microscopes (SEMs) Philips XL30 and Tescan VEGA TS 5130MM, equipped with an energy-dispersive X-ray spectroscopy (EDS) Oxford Instruments INCA. X-Ray powder diffraction (XRD) analysis of the cobalt powders was realized using a PHILIPS PW 1050 diffractometer. Magnetic measurements were performed using a Quantum Design MPMS SQUID magnetometer at temperatures of 5 K and 300 K.

RESULTS AND DISCUSSION

Morphology and structure analysis

Due to parallelism between reactions of cobalt electrodeposition and hydrogen evolution,[18] the hydrogen generated during the electrodeposition process strongly affected the morphology of the powder particles. The quantity of hydrogen evolved parallel with the process of metal deposition was quantified by the determination of the current efficiency for hydrogen evolution using a well-established experimental procedure.[19] The polarization characteristics of a electrolyte containing 0.1 M $CoSO_4$ +1 M $(NH_4)_2SO_4$ + 0.7 M NH_4OH were previously analyzed, and it was concluded that a current density of 770 mA cm^{-2} corresponded to the limiting diffusion current density for Co electrodeposition ($j_{L(Co)}$ = 770 mA cm^{-2}).[20] The values of the current efficiencies for the Co electrodeposition of 18 and 26 % were extracted from the polarization curve obtained with IR drop correction at 770 and 500 mA cm^{-2}, respectively. Hence, the current efficiencies for hydrogen evolution reaction at these current densities were 82 ($j_{L(Co)}$ = 770 mA cm^{-2}) and 74 % (j = 500 mA cm^{-2}). Typical powder particles of cobalt obtained at a current density of 500 and at a current density corresponding to the limiting diffusion current density for Co electrodeposition of 770 mA cm^{-2} are shown in Figs. 1 and 2, and denoted Co1 and Co2, respectively. The observed powder particles were either dendritic or spongy-like shapes. A mixture of dendritic and spongy-like particles was formed at a current density of 500 mA cm^{-2}, while only the spongy-like particles were formed at the limiting diffusion current density of 770 mA cm^{-2}.

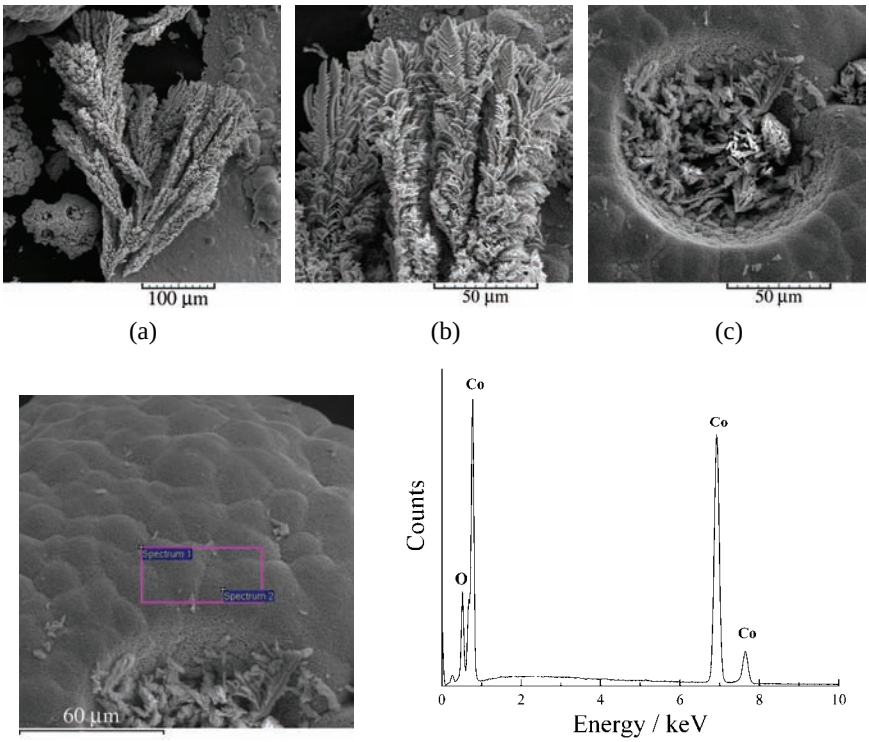

Fig. 1. Morphology of cobalt powder particles obtained by electrodeposition at a current density of 500 mA cm^{-2} (Co1): a) dendrite and spongy-like particles, b) dendrite, c) dendrites formed inside holes, d) structure of grains around hole and e) EDS spectrum of the as-deposited powder.

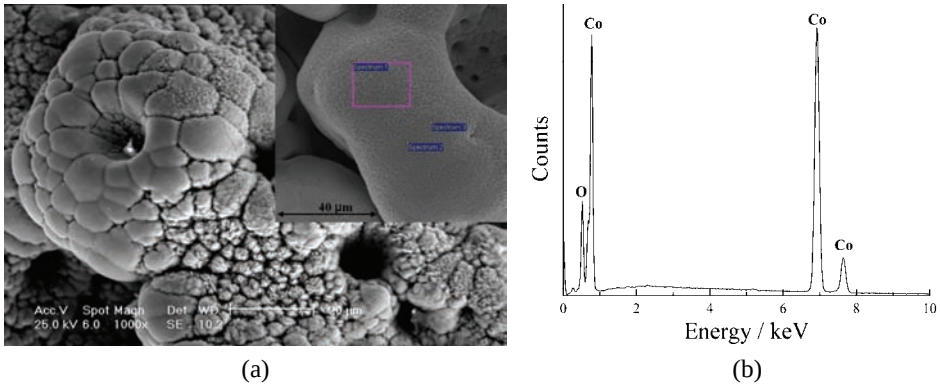

Fig. 2. Morphology of cobalt powder particles obtained by electrodeposition at a current density corresponding to the limiting diffusion current density of 770 mA cm^{-2} (Co2): a) spongy-like particle with magnified details of the surface and b) EDS spectrum of the as-deposited powder.

The cobalt dendrites have the 3D (three-dimensional) fern-like shape (Fig. 1a and b). The cobalt dendrites were also formed in the interior of most holes after the detachment hydrogen bubbles, as shown in Fig. 1c. Regarding the spongy-like particles obtained at 500 mA cm^{-2}, it can be noticed that the spongy character of this particle type is determined by holes formed by detached hydrogen bubbles surrounded by cauliflower-like agglomerates of cobalt grains. The morphology surface of cobalt grains around holes was relatively smooth with numerous nano pores, as shown in Fig. 1d and e shows the energy dispersion spectroscopy (EDS) measurement of the as-deposited powder. A slight peak of oxygen exists, which indicates that the surface of the powder has a quite thin oxide layer due to the passivation of cobalt.

The macrostructure of the spongy-like particles obtained at 770 mA cm^{-2} (Co2) resembled that of those obtained at 500 mA cm^{-2} (Co1, Fig. 2a). Due to vigorous hydrogen evolution during the formation of these particles, small holes inside larger holes were also formed (enlarged part in Fig. 2a). The morphology of the deposits between the holes also (Fig. 2a) consisted of small agglomerates of cobalt grains separated by irregular micro-pores, the origin of which was also due to the hydrogen generated during the electrodeposition process. The morphology of grains around holes was relatively smooth with numerous nano-pores (enlarged parts in Fig. 2a). As in the previous case, there was a quite thin oxide layer on the surface of the powder due to the passivation of cobalt (Fig. 2b).

The effect of hydrogen evolution, as a parallel reaction to cobalt electrodeposition, on the shape of powder particles could be explained as follows: in the case of the formation of dendritic particles, the evolved hydrogen prevented the growth of the dendrites in the lateral directions causing a predominant growth in the vertical direction in the stem-like form, as shown in Fig. 1a and b. The growth of a dendrite commenced from one nucleus (Fig. 1a) and then, the growth of the dendritic particle was determined by the hydrogen evolution reaction. Hydrogen evolution intensified with increasing current density of the electrodeposition leading to inhibition of dendritic growth. Hydrogen evolution became sufficiently vigorous to cause strong stirring of the electrolyte in the near-electrode layer leading to a decrease in the thickness of the diffusion layer, an increase in the limiting diffusion current density and a decrease in the degree of diffusion control of the electrodeposition process.[21] The absence of dendritic-shaped particles in the deposit obtained at 770 mA cm^{-2} actually proved that the degree of diffusion control was lower during electrodeposition at 770 mA cm^{-2} than at 500 mA cm^{-2} due to the intensification of the hydrogen evolution reaction. The quantity of evolved hydrogen during the electrodeposition process can be divided into two parts.[22] One part is spent for the creation of macro-pores or holes and determines the overall specific surface area of the spongy-like particles. This quantity of generated hydrogen does not contribute to the stirring of electrolyte in

the near-electrode layer. The remaining quantity of evolved hydrogen was responsible for the stirring of the electrolyte and, hence, affected the hydrodynamic conditions in the near-electrode layer. The morphology of the spongy-like particles was determined by this remaining quantity of evolved hydrogen, which was also responsible for the formation of the porous structure of this type of particles, *i.e.*, the formation of micro- and nano pores.

The crystal phase composition

The crystallinity and phase composition of the obtained cobalt powders were determined from the XRD patterns depicted in Fig. 3 in the 2θ range of 40–60°. The peak positions of sample Co1 were located at 2θ angles 41.69, 44.60 and 47.52°. The peak positions and intensity ratios matched the corresponding (100), (002) and (101) reflections related to the hexagonal-close packed (hcp) cobalt phase (space group P63/mmc1 (194); JCPDS: 05-0727). No reflections due to cobalt oxides or hydroxides impurities were detected, indicating that the cobalt powder obtained in this way consisted of only the hcp-Co phase. In the case of Co2 sample, notable changes in breadths and relative intensities of the peaks were observed (Fig. 3). Significant broadening of the peaks in this case suggests increased defect concentration (microstrain), as a consequence of the synthesis conditions for this sample. The notable increase in the relative intensity of the (002) peak at 44.60° in Co2 was inconsistent with the XRD pattern of a single hcp phase and pointed to the contribution of the fcc-Co phase through its strongest (111) reflection at the same 2θ angle (space group Fm-3m (225), JCPDS: 15-0806).[23] The detection of both structure phases in the Co2 sample was also in accordance with the higher defect concentration, since it is known that their presence favours the simultaneous existence of hcp and fcc structures in bulk cobalt.[14]

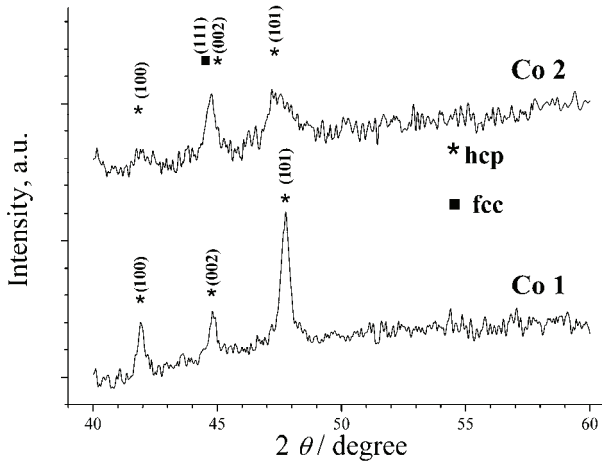

Fig. 3. XRD patterns of cobalt powders deposited at 500 (Co1) and 770 mA cm^{-2} (Co2).

Magnetic properties

Magnetic properties of two cobalt samples were investigated by measurements of field dependence of isothermal magnetization at two temperatures, 5 and 300 K. The recorded magnetization curves in the magnetic field interval of ±50 Oe are depicted in Fig. 4a and b for Co1 and Co2, respectively, while the insets show low-field details of the hysteresis loops. The most important parameters extracted from the obtained M(H) dependencies are listed in Table I. The saturation magnetization M_S values were considered as the measured values in the maximum field of 50 Oe while the coercivity fields H_C were determined as the interpolated field value for zero sample magnetization.

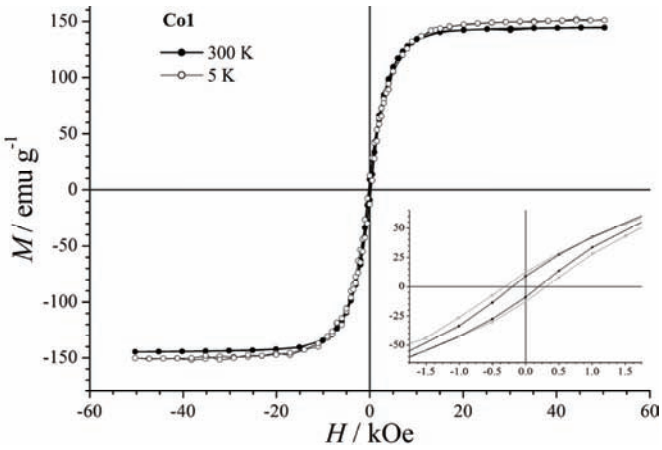

(a)

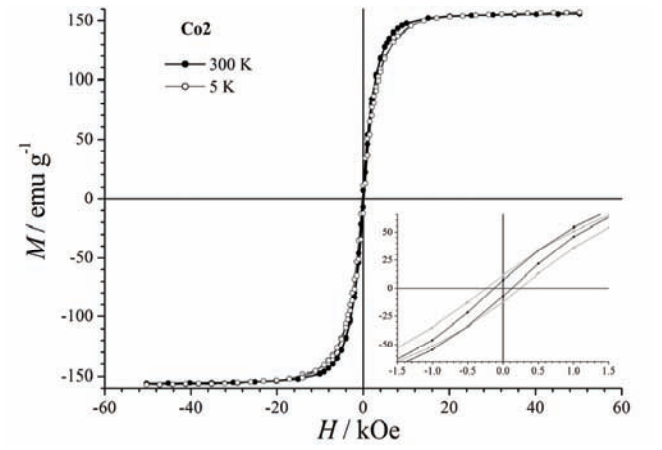

(b)

Fig. 4. Hysteresis loops of cobalt powder electrodeposited at a) 500 (Co1) and b) 770 mA cm^{-2} (Co2) at 5 and 300 K; in insets are the details of the hysteresis loops.

TABLE I. Magnetic parameters for both samples obtained from the *M*(H) curves at two measurement temperatures

Sample	Temperature, K	
	5	300
Co1	M_S = 151 emu g^{-1} H_C = 300 Oe	M_S = 144 emu g^{-1} H_C = 200 Oe
Co2	M_S = 157 emu g^{-1} H_C = 220 Oe	M_S = 156 emu g^{-1} H_C = 160 Oe

The obtained magnetic behaviour of both samples was typical for soft ferromagnetic material that saturates in low to moderate applied fields, and possesses a narrow hysteresis loop. The obtained values of the saturation magnetization M_S were lower than for bulk cobalt (168 emu g^{-1}), which is consistent with the findings of the EDS experiments indicating to the presence of small amount of a cobalt oxide passivation layer at the sample surface. Cobalt oxide possesses antiferromagnetic ordering up to the room temperature,[13] and, consequently, its contribution to the magnetic moment of the material was negligible. Nevertheless, the obtained values of saturation magnetization are among the highest with respect to the values reported in the literature for three-dimensional cobalt structures.[6,24]

Obtained H_C values for both samples were larger than typical literature values for bulk cobalt, while they were similar to these found for other cobalt structures with different morphologies.[1,6,25] It was shown that coercivity predominantly depends on the crystallinity and morphology of materials, so the obtained difference between the Co1 and Co2 samples was understandable. It should be noted that the coercivity of sample Co2 was lower than that of sample Co1, which is in compliance with the findings from both the XRD patterns and the SEM analysis. Namely, from the XRD data, it was concluded that the Co1 sample consisted of pure hcp cobalt phase, while the Co2 sample, besides hcp phase, also contained fcc cobalt phase, which is magnetically softer than hcp phase. In addition, the lower morphological diversity found in Co2 by the SEM analysis could also have caused a decrease of the magnetic anisotropy in the system, which consequently led to a lower H_C value.

An additional interesting point resulting from a comparison of the obtained behaviour of coercivity and saturation magnetization at 5 and 300 K (data in Fig. 4a and b): both H_C and M_S decreased faster with temperature for Co1 than for Co2. In fact, M_S for sample Co2 was virtually the same at 5 and 300 K. A known peculiarity of bulk cobalt magnetism is the increase of its critical ferromagnetic (Curie) temperature T_C with amorphization of the crystal structure, which was demonstrated both experimentally and theoretically.[26,27] It was shown that T_C increased by several hundreds degrees for amorphous cobalt in comparison to well-crystallized bulk cobalt. The present results are in accordance with these

findings since H_C decreased faster with temperature for the well-crystallized sample Co1, while M_S remained almost constant up to 300 K for the poorly crystallized sample Co2.

Correlation between morphology and magnetic properties

Although the values of saturation magnetization M_S for the powder particles obtained at the both current densities were lower than that for the bulk cobalt, it is necessary to note that the value for the particles obtained at 770 mA cm^{-2} was closer to the value for bulk cobalt, which could be explained as follows: the powder particles produced at 770 mA cm^{-2} were obtained under conditions of more vigorous hydrogen evolution than those obtained at 500 mA cm^{-2}. From the viewpoint of the electrodeposition process, this means that potential at which the electrodeposition process really occurred was lower at the current density of 770 mA cm^{-2} than at 500 mA cm^{-2} (the concept of "effective overpotential" or "effective potential").[21] This means a decrease in the degree of diffusion control of electrodeposition process with intensification of hydrogen evolution. As a consequence, the morphologies of deposits became similar to those obtained at lower potentials or current densities, at which hydrogen evolution is less vigorous. This process led to an increase in the compactness of the particles and the structure of these particles approached the structure characteristic for bulk Co.[18]

As already mentioned, the dendritic growth was completely inhibited by the hydrogen evolution reaction during electrodeposition at 770 mA cm^{-2}. The specific surface area of particles obtained in such a manner (cauliflower-like or spongy-like particles) was smaller than that of dendritic particles.[28] Due to smaller specific area of the spongy-like particles, the surface area of these particles was less exposed to air and, hence, to the creation of oxide at their surface than dendritic particles. In this way, the better magnetic characteristics of the particles obtained at 770 mA cm^{-2} than those obtained at 500 mA cm^{-2} may be explained.

CONCLUSIONS

The experimental results demonstrated that it was possible to control the morphology, structure and magnetic properties of cobalt 3D powder particles by adjusting process parameters of electrodeposition such as current density. Dendrites and spongy-like particles were obtained at a current density of 500 mA cm^{-2}, while the only the spongy-like particles were produced by electrodeposition at 770 mA cm^{-2}. XRD analysis indicated that the cobalt powder obtained at 500 mA cm^{-2} consisted of single phase hcp-Co phase but in the cobalt powder sample electrodeposited at 770 mA cm^{-2}, both structure phases of cobalt, hcp and fcc, were detected. The values of obtained saturation magnetization were lower than that for bulk cobalt (168 emu g^{-1}), which is consistent with the findings of the EDS experiments that pointed to the presence of a small amount of a

cobalt oxide passivation layer at the surface of the samples. The enhanced values of coercivity were the result of increased magnetic anisotropy caused by the peculiar morphologies of the powder particles.

Acknowledgment. This work was financially supported by the Ministry of Education, Science and Technological Development of the Republic of Serbia under Grant No. III 45012.

И З В О Д

МЕЂУСОБНА ПОВЕЗАНОСТ МОРФОЛОГИЈЕ И МАГНЕТНИХ СВОЈСТАВА ЧЕСТИЦА ЕЛЕКТРОХЕМИЈСКИ ПРОИЗВЕДЕНОГ ПРАХА КОБАЛТА

ВЕСНА М. МАКСИМОВИЋ[1], НЕБОЈША Д. НИКОЛИЋ[2], ВЛАДАН Б. КУСИГЕРСКИ[1] и ЈОВАН Л. БЛАНУША[1]

[1]Институт за нуклеарне науке „Винча“, Универзитет у Београду, Београд и [2]ИХТМ – Центар за електрохемију, Универзитет у Београду, Његошева 12, Београд

3Д честице праха кобалта су добијене галваностатским таложењем. Електрохемијски исталожен прах кобалта карактерисан је рендгено-дифракционом анализом, техником скенирајуће електронске микроскопије и енергетско-дисперзионом спектроскопијом, као и помоћу SQUID магнетометра. Показано је да су морфологија, структура и магнетна својства честица кобалта тесно повезане и да се могу лако контролисати подешавањем електрохемијских параметара. У зависности од примењене густине струје формирају се две врсте честица праха: дендрити при ниским и сунђерасте честице при вишим вредостима густине струје. Морфологија и структура честица су у међусобној вези са магнетним својствима, а поређене су и са својствима „*bulk*“ кобалта. У поређењу са „*bulk*“ кобалтом, добијене 3Д структуре показују смањену сатурациону магнетизацију (M_S), али побољшану коерцитивност (H_C), што се објашњава њиховом неуобичајеном морфологијом.

(Примљено 20. август, ревидирано 8. октобра, прихваћено 24. октобра 2014)

REFERENCES

1. Z. Lu-Ping, X. Hong-Mei, Z. Wei-Dong, Y. Yang, F. Shao-Yun, *Cryst. Growth Des.* **8** (2008) 1113
2. M. Rivera, C. H. Rios-Reyes, L. H. Medoza-Huizar, *Appl. Surf. Sci.* **255** (2008) 1754
3. A. B. Soto, E. M. Arce, M. Polimar-Pardave, I. Gonzalez, *Electrochim. Acta* **41** (1996) 2647
4. N. Pradhan, P. Singh, B. C. Tripathy, S. C. Das, *Miner. Eng.* **14** (2001) 775
5. H. Cao, L. Wang, Y. Qui, Q. Wu, G. Wang, L. Zhang, X. Liu, *Chemphyschem* **7** (2006) 1500
6. X. Liu, R. Yi, Y. Wang, G. Qui, N. Zhang, X. Li, *J. Phys. Chem. C* **111** (2007) 163
7. V. D. Jović, N. D. Nikolić, U. Č. Lačnjevac, B. M. Jović, K. I. Popov, in *Electrochemical Production of Metal Powders*, Series: *Modern Aspects of Electrochemistry*, S. S. Djokić, Ed., Vol. 54, Springer, Berlin, 2012, p. 63
8. M. Erbudak, E. Wetli, M. Hochstrasser, D. Pescia, D. D. Vvedensky, *Phys. Rev. Lett.* **79** (1997) 1893
9. O. Kitakami, H. Sato, Y. Shimada, F. Sato, M. Tanaka, *Phys. Rev., B* **56** (1997) 13849
10. H. Sato, O. Kitakami, T. Sakurai, Y. Shimada, Y. Otani, K. Fukamichi, *J. Appl. Phys.* **81** (1997) 1858
11. V. V. Matveev, D. A. Baranov, G. Y. Yurkov, N. G. Akatiev, I. P. Dotsenko, S. P. Gubin, *Chem. Phys. Lett.* **422** (2006) 402

12. Y. Song, H. Modrow, L. L. Henry, C. K. Saw, E. Doomes, V. Palshin, J. Hormes, C. S. S. R. Kumar, *Chem. Mater.* **18** (2006) 2817
13. A. Oles, F. Kajzar, M. Kucab, W. Sikora, *Magnetic Structures*, Panstwowe Wydawnictwo Naukowe, Krakow, 1976
14. S. Sun, C. B. Murray, *J. Appl. Phys.* **85** (1999) 4325
15. K. I. Popov, S. S. Djokić, B. N. Grgur, *Fundamental aspects of electrometallurgy*, Kluwer Academic/Plenum Publishers, New York, 2002, p. 1
16. N. D. Nikolić, V. M. Maksimović, G. Branković, P. M. Živković, M. G. Pavlović, *J. Serb. Chem. Soc.* **78** (2013) 1387
17. R. Winand, *Electrochim. Acta* **39** (1994) 1091
18. V. D. Jović, V. M. Maksimović, M. G. Pavlović, K. I. Popov, *J. Solid State Electrochem.* **10** (2006) 373
19. N. D. Nikolić, K. I. Popov, Lj. J. Pavlović, M. G. Pavlović, *J. Electroanal. Chem.* **588** (2006) 88
20. V. D. Jović, B. M. Jović, M. G. Pavlović, *Electrochim. Acta* **51** (2006) 5468
21. N. D. Nikolić, K. I. Popov, in *Electrodeposition: Theory and Practice*, Series: *Modern Aspects of Electrochemistry*, S. S. Djokić, Ed., Vol. 48, Springer, Berlin, 2010, p. 1
22. N. D. Nikolić, G. Branković, M. G. Pavlović, *Powder Technol.* **221** (2012) 271
23. E. A. Owen, D. Madoc Jones, *P. Phys. Soc., B* **67** (1954) 456
24. G. Dumpich, T. P. Krome, B. Hausmanns, *J. Magn. Magn. Mater.* **248** (2002) 241
25. H. L. Niu, Q. W. Chen, H. F. Zhu, Y. S. Lin, X. Zhang, *J. Mater. Chem.* **13** (2003) 1803
26. K. Fukamichi, T. Goto, U. Mizutani, *IEEE Trans. Magn.* **MAG-23** (1987) 3590
27. Y. Kakehashi, *Phys. Rev., B* **43** (1991) 10820
28. N. D. Nikolić, K. I. Popov, in *Electrochemical Production of Metal Powders*, Series: *Modern Aspects of Electrochemistry*, S. S. Djokić, Ed., Vol. 54, Springer, 2012, p. 125.